Int J Thermophys (2017) 38:156
DOI 10.1007/s10765-017-2289-4

TEMPMEKO 2016

Estimating Surface Temperature of a Calibration Apparatus for Contact Surface Thermometers from Its Internal Temperature Profile

I. Saito[1] · **T. Nakano**[1] · **J. Tamba**[1]

Received: 31 August 2016 / Accepted: 16 August 2017 / Published online: 31 August 2017

Abstract A calibration apparatus for contact surface thermometers was developed. Temperature of the upper surface of a copper cube of the calibration apparatus was used as reference surface temperature, which was estimated at around 50 °C, 100 °C, and 150 °C by not only two conventional industrial platinum resistance thermometers (IPRTs) but also five small-sized platinum resistance thermometers (SSPRTs) calibrated based on the International Temperature Scale of 1990 (ITS-90). These thermometers were inserted horizontally into the copper cube and aligned along the center axis of the copper cube. In the case of a no-load state without anything on the upper surface, the temperature profile inside the copper cube linearly decreased from the lower part to the upper surface, which suggests that the heat conduction inside the copper cube can be regarded as a one-dimensional steady state. On the other hand, in the case of a transient state just after the contact surface thermometer was applied to the upper surface, the temperature profile became a round shape. We obtained good agreement between the curvature of the temperature profiles and the results estimated by using an error function used for a one-dimensional transient heat conduction problem. The temperature difference between the estimated temperature by linear extrapolation using two IPRTs and that by extrapolation using the error function was within 0.2 °C in the transient state at around 150 °C. Over 10 min after the contact surface thermometer was applied, the temperature profile showed a linear shape again, which indicated that linear extrapolation using two IPRTs was well for the estimation of the reference sur-

Selected Papers of the 13th International Symposium on Temperature, Humidity, Moisture and Thermal Measurements in Industry and Science.

✉ I. Saito
saitou.19hiko@aist.go.jp

[1] National Metrology Institute of Japan (NMIJ), National Institute of Advanced Industrial Science and Technology (AIST), AIST Tsukuba Central 3, 1-1-1 Umezono, Tsukuba 305-8563, Japan

face temperature because the heat conduction state inside the copper cube came back to the one-dimensional steady state. Difference between the surface temperature and temperature detected by the contact surface thermometer was also observed after the contact surface thermometer touched on the upper surface. The difference was over 0.1 °C at several minutes after the contact surface thermometer touching on the reference surface and was suppressed with passing time in the transient state and became negligible over 10 min.

Keywords Calibration apparatus · Measurement uncertainty · Surface temperature measurement · Surface thermometer

1 Introduction

Many industries require measurement of the surface temperature of products and/or heating equipment. For example, surface temperature of steels is observed during some manufacturing processes; surface temperature of hot plates is checked for keeping quality of food processing. To measure the surface temperature, contact surface thermometers are widely used because of their simple and easy operation. These industries also require calibration or check of the contact surface thermometers based on the International Temperature Scale of 1990 (ITS-90) [1] to maintain reliability of the temperature measurements.

Over the past ten years, several institutes have developed apparatuses to calibrate contact surface thermometers [2–12]. These thermometers were calibrated by comparing their indicated temperature to a reference surface temperature, which was determined at an upper surface of a metal block in the calibration apparatuses. In the previous studies, the reference surface temperature was estimated by linear extrapolation of temperatures from inside of the metal block to the reference surface using two or three thermometers inserted into the metal block [3–5].

Although the linear extrapolation is simple and usable for the estimation of the reference surface temperature, there may be some discrepancy between the reference temperature estimated by the linear extrapolation and a surface temperature estimated by observing much more detailed temperature profile inside of a metal block. So far, observation of a detailed temperature profile of an inside metal block has been superficial to estimate the reference for the calibration apparatus for contact surface thermometers.

In this study, we developed a calibration apparatus consisting of a copper cube, of which the upper surface of the cube was used as the reference surface. To observe temperature profile from the inside of the copper cube to the upper surface in detail, we inserted not only two conventional industrial platinum resistance thermometers (IPRTs) but also five small-sized platinum resistance thermometers (SSPRTs), which are traceable to the ITS-90, in the copper cube. These thermometers were aligned along the center axis of the copper cube and provided precise temperature profile inside of the copper cube.

In this study, firstly, we will describe linear features of the temperature profile inside the copper cube in the case of a no-load state, namely no contact surface thermometer

on the reference surface, by using both the IPRTs and SSPRTs around 50 °C, 100 °C, and 150 °C. The uncertainties of the estimation of the upper surface temperature were also shown.

Secondly, we will describe a round shape of a temperature profile in a transient state. Then, difference between a surface temperature obtained by the linear extrapolation using two IPRTs and that estimated by the round shape will be discussed.

We also observed the time variation of the upper surface temperature and the output of the surface thermometer over 30 min through the surface thermometer was applied to the upper surface around 150 °C. Finally, we will present preliminary results for differences in the surface temperature and the output of the surface thermometer in the transient state.

In this study, our main scope is observation of a detailed temperature profile of the copper cube for estimation of the reference surface temperature of the calibration apparatus. Thus, this study is limited to the estimation of reference surface temperature in the calibration laboratories, where the ambient conditions are very stable to exclude effects of outside condition on the temperature of reference surface.

2 Experimental

2.1 Calibration Apparatus of the Surface Thermometer

Figure 1 shows a schematic side view of the calibration apparatus. The main part of the apparatus consists of an oxygen-free high conductivity copper cube, where one side is 100 mm. It is plated with nickel to prevent oxidation. It is covered with a heat insulator except for the upper surface, where a contact surface thermometer touches. The temperature of the copper cube is controlled to a certain value by using a thermometer and a heater. The heater, of which the output power was 900 W, is installed in the lower part, and the thermometer used for controlling temperature is inserted just above the heater at a depth of 67 mm from the upper surface.

The temperature profile in the copper cube was measured by using two types of platinum resistance thermometers (PRTs). First type of PRT was the conventional IPRT with an indicator (Model APT-100, Anritsu Meter) as shown in Fig. 2a; the sensing

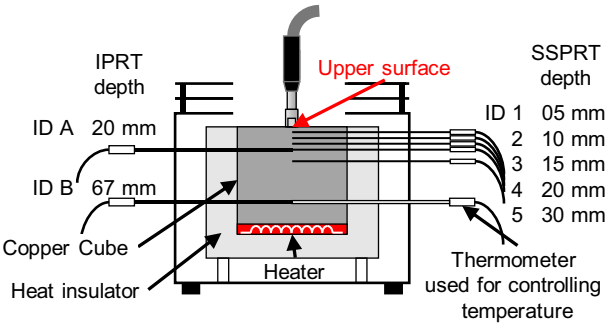

Fig. 1 Schematic side view of the calibration apparatus

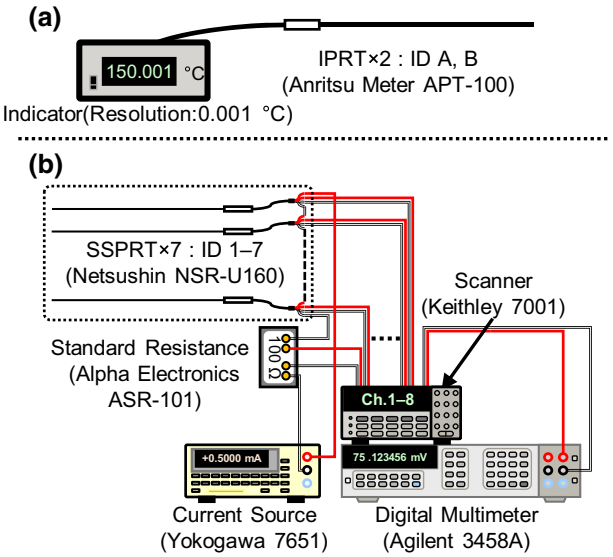

Fig. 2 Schematic diagrams of (a) IPRTs with the measurement instrument, and (b) connections between SSPRTs and measurement devices

element was about 100 Ω at 0 °C, the diameter was 3.2 mm, the length was 50 cm, the resolution of indicator was 0.001 °C, and the minimum time interval for temperature measurement is 1 s. Two IPRTs were used (ID A and ID B) in this study. As shown in Fig. 1, the IPRT ID B was inserted at depths of 67 mm from the upper surface, which was the same depth of the thermometer used for controlling temperature to check reliability of the thermometer used for controlling temperature during the calibration. On the other hand, the IPRT ID A was inserted at depth of 20 mm from the upper surface to estimate the surface temperature using conventional liner extrapolation of the two thermometers, namely IPRTs ID A and ID B.

Second type of PRT was the SSPRT, which was Netsushin NSR-U160; the diameter was 1mm, the length was 60 cm, and the resistance at TPW (R_{TPW}) was 100 Ω. In this study, as shown in Fig. 1, SSPRTs were inserted horizontally from the opposite side of the IPRTs. To check more detail temperature profile between the upper surface and the IPRT ID A, four SSPRTs (ID 1–ID 4) were inserted at depths of 5 mm, 10 mm, 15 mm, and 20 mm, respectively, from the upper surface to the IPRT ID A. We also inserted an SSPRT ID 5 at 30 mm from the upper surface to obtain the information of the temperature profile between IPRTs ID A and ID B. Two SSPRTs ID 6 and ID 7 were also inserted at the same depth as the SSPRT ID 1 from the upper surface. They ran parallel to the SSPRT ID 1 at a distance of 40 mm on the right and left sides to estimate the temperature distribution of the upper surface. Characteristics of the SSPRT have been evaluated in detail by the National Metrology Institute of Japan (NMIJ)/National Institute of Advanced Industrial Science and Technology (AIST) up to temperature of the freezing point of Indium (156.5985 °C) [13]. So, in this study, the temperature profiles of the calibration apparatus were observed around 50 °C, 100 °C, and 150 °C below the freezing point of Indium.

2.2 Measurement Method of SSPRTs and IPRTs

Figure 2b shows a schematic diagram of the connections between the SSPRTs and measurement devices. All of SSPRTs and a standard resistor (100 Ω) were connected in series, and 0.5 mA electric current was constantly applied by a current source (Model 7651, Yokogawa Meters & Instruments). We selected each SSPRT or the standard resistor by using a scanner (Model 7001, Keithley Instruments) to measure voltage induced by the SSPRTs and the standard resistor using a digital multimeter (Model 3458A, Agilent Technologies). All measurement devices were controlled by a personal computer. The whole time period for one scanning series of the seven SSPRTs and the standard resistor was set within 1 s to observe the transient response of the temperature profile just after the surface thermometer was applied.

To obtain the resistance of the SSRPTs, we used the following formula:

$$R_{\mathrm{PRT},i} = \frac{V_{\mathrm{PRT},i}}{V_{\mathrm{std}}} \times R_{\mathrm{std}}, \tag{1}$$

where $V_{\mathrm{PRT},i}$ and V_{std} are voltages of the SSPRTs and the standard resistor, respectively, obtained by the digital multimeter; $R_{\mathrm{PRT},i}$ and R_{STD} are the resistances of the SSPRTs and the standard resistor, respectively; and i is the ID number of the SSPRTs. R_{STD} was calibrated to be traceable to the national standard of resistance at NMIJ/AIST.

The self-heating effect for the SSPRTs in the copper cube was observed by pre-measurements using two currents of 0.5 mA and $0.5\sqrt{2}$ mA. The self-heating was estimated to be about 5 mK at 0.5 mA for the SSPRTs. In this study, the results for each SSPRT are given for a zero thermometer current by correcting the self-heating estimated by the pre-measurements.

On the other hand, the current of the indicator of each IPRT (ID A, B) was fixed at 1 mA. So, it was difficult to estimate the size of the self-heating for each IPRT at 1 mA using the indicator in the same way as that for SSPRTs. Thus, in this paper, the measurement results are given at 1 mA for IPRTs. However, we observed the size of self-heat at 1 mA for this type of IPRT using a different current source and a digital multimeter. The size of self-heating was estimated to be within 0.06 °C at 1 mA.

2.3 Calibration of SSPRTs and IPRTs

All of the SSPRTs and the IPRTs were calibrated in order to be traceable to ITS-90 at 50 °C, 100 °C, and 150 °C by comparing them with a reference thermometer calibrated at NMIJ/AIST. The reference thermometer is a standard platinum resistance thermometer (SPRT), which was calibrated at triple point of water (TPW) and the freezing point of indium before the comparison measurements. In order to obtain an stable temperature state for the comparison measurements, we used a pressure control heat pipe developed in NMIJ/AIST [14]. The temperature stability was within 0.1 mK, as reported before [14]. The stability of the SSPRTs and the IPRTs during calibration

Table 1 Uncertainty budget for the calibration of SSPRTs and IPRTs using the pressure control heat pipe at around 150 °C

Uncertainty components (°C)	SSPRTs	IPRTs
1. Stability of PRT in the calibration—$u_{\mathrm{cal,stb}}$	0.002	0.001
2. Deviation of measurement—$u_{\mathrm{cal,dev}}$	0.001	0.001
3. Self-heating effect—$u_{\mathrm{cal,self}}$	0.001	0.03
4. Reference thermometer (SPRT)—$u_{\mathrm{cal,sprt}}$	0.002	0.002
5. Measurement instrument—$u_{\mathrm{cal,mi}}$	0.002	0.001
Combined standard uncertainty ($k = 1$)—u_{cal}	0.004	0.03
Expanded uncertainty ($k = 2$)—U_{cal}	0.008	0.06

was also evaluated by taking measurements at the triple point of water (TPW) before and after calibration.

To calibrate the SSPRTs and the IPRTs, we used the same devices and connection as shown in Fig. 2. Table 1 presents the uncertainty budget for the calibration at 150 °C. Each uncertainty component in Table 1 is described below:

1. Stability of PRT in the calibration—$u_{\mathrm{cal,stb}}$: The first component was evaluated according to the difference in measured values for each thermometer at the TPW before and after the calibration.
2. Deviation of measurement—$u_{\mathrm{cal,dev}}$: The second component was estimated from the experimental standard deviation of the resistance measurement at calibration temperature.
3. Self-heating effect—$u_{\mathrm{cal,self}}$: The third component was an uncertainty due to the self-heating. The self-heating effect for SSPRT was evaluated by measurements using two currents of 0.5 mA and $0.5\sqrt{2}$ mA. On the other hand, since the size of self-heating was estimated to be within 0.06 °C at 1 mA for the IPRTs, the uncertainty of self-heating for the IPRTs was evaluated on the assumption of a rectangular distribution of the size of the self-heat estimated at 1 mA.
4. Reference thermometer (SPRT)—$u_{\mathrm{cal,sprt}}$: The fourth component was the uncertainty due to the measurement of SPRT as the reference thermometer for the calibration of the SSPRTs and the IPRTs. The uncertainty component also included not only an uncertainty due to calibration of the SPRT itself and also the stability of the SPRT during comparison measurements. Details of the measurement of SPRTs using the pressure control heat pipe were described in the former report [14].
5. Measurement instrument—$u_{\mathrm{cal,mi}}$: The last component was the uncertainty due to measurement instruments. It considers the following items: the calibration uncertainty of the reference resistance, the stability of the digital multimeter and the current source for the SSPRTs, and a resolution of the indicator for the IPRTs.

The expanded uncertainties of the calibration for the SSPRTs and the IPRTs were 0.008 °C and 0.06 °C, respectively. The uncertainties of the calibration for the SSPRTs and the IPRTs at 50 °C and 100 °C were almost the same as that at 150 °C. We also measured the SPPRTs and the IPRTs at additional two temperature points in the vicinity

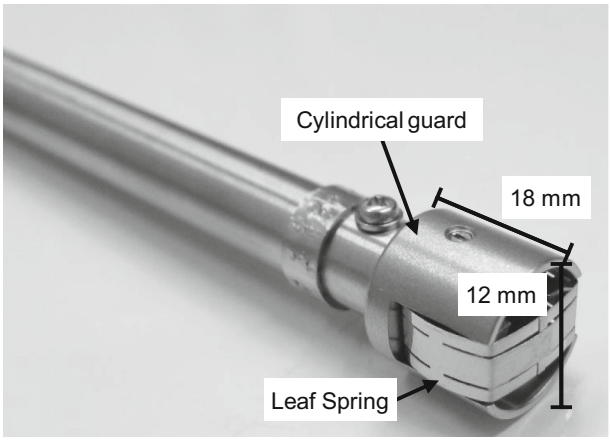

Fig. 3 Contact surface thermometer used in this study

of 50 °C, 100 °C, and 150 °C using the same procedure of the calibration in order to obtain their sensitivity.

2.4 Surface Thermometer

Figure 3 shows a surface thermometer (Model A series, Anritsu Meter) used in this study. The thermometer has a length of 10 cm. The sensing element is a type K thermocouple. Compensating wires were not used for the surface thermometer between hot and cold junctions. The cold junction was realized with a water–ethanol bath at 0 ° C. The type K thermocouple was attached behind a leaf spring. A cylindrical guard made of stainless steel surrounded the leaf spring to make the leaf spring contact on a surface of something under temperature measurement satisfactorily.

We have also used a dedicated device in order to touch the contact surface thermometer well on the reference surface automatically and to exclude human error for the touching procedure. This device enables us better repeatability of the measurements and long-term measurements for over 30 min though the surface thermometer touching on the calibration apparatus.

3 Results and Discussion

3.1 Temperature Profile Inside the Copper Cube of the Calibration Apparatus in the No-Load State

Figure 4a–c shows the temperature profiles inside the copper cube of the calibration apparatus in the no-load state without anything on its surface at around 50 °C, 100 °C, and 150 °C, respectively. The error bar at each measurement point for the SSPRTs and the IPRTs represents the expanded uncertainty ($k = 2$). Table 2 presents the

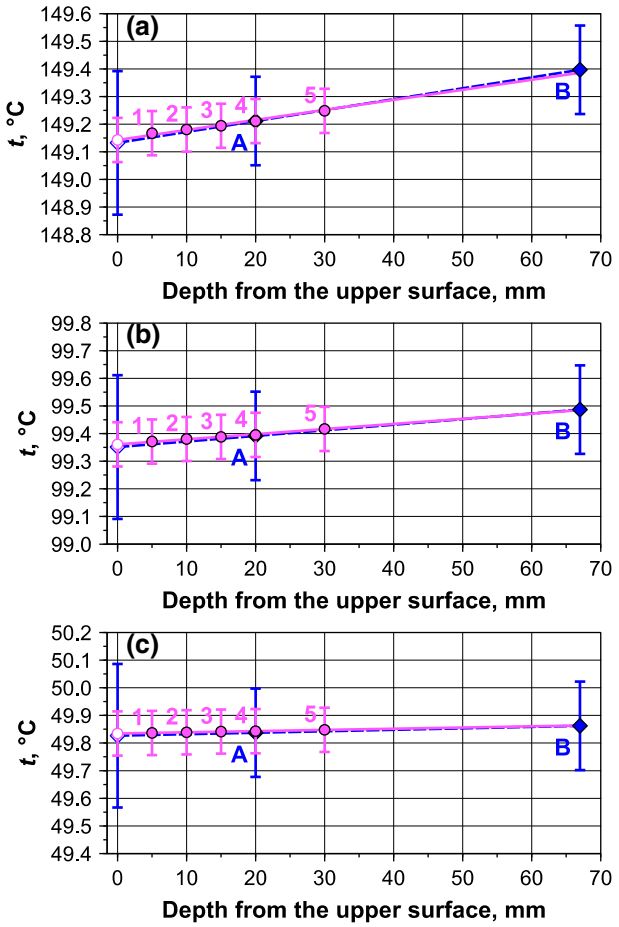

Fig. 4 Temperature profiles inside the copper cube in the no-load state at (a) 150 °C, (b) 100 °C, and (c) 50 °C. The *solid line* and the *broken line linear line* are obtained by using five SSPRTs (ID 1–ID 5) and one IPRT (ID B) and using two IPRTs (ID A and ID B), respectively. The surface temperatures estimated by using two IPRTs (ID A and ID B), $t_{A,B}$, and by using five SSPRTs (ID 1–ID 5) and one IPRT (ID B), t_{1-5+B}, are also shown at 0 mm and by *outlined symbols*. The *error bars* are the expanded uncertainty ($k = 2$) estimated for each point and surface temperature

uncertainty budget for the measurement of the SSPRTs and the IPRTs at around 150 °C. Each uncertainty component in Table 2 is described below:

1. Calibration—u_{cal}: The first component was the uncertainty of calibration for each thermometer as described in Table 1.
2. Long-term drift—$u_{nl,drift}$: The second component was evaluated according to difference in measured values for each thermometer at the TPW before and after the temperature profile measurement.
3. Deviation of measurement—$u_{nl,dev}$: The third component was estimated from the width of deviation of measurements for 15 min which was within 0.03 °C.

Table 2 Uncertainty budget of the temperature measurement for SSPRTs and IPRTs in the no-load state at around 150 °C

Uncertainty component (°C)	SSPRTs	IPRTs
1. Calibration—u_{cal}	0.004	0.03
2. Long-term drift—$u_{\mathrm{nl,drift}}$	0.005	0.005
3. Deviation of measurement—$u_{\mathrm{nl,dev}}$	0.01	0.01
4. Self-heating effect—$u_{\mathrm{nl,self}}$	0.02	0.03
5. Position of the sensing element and Heat flux—$u_{\mathrm{nl,position}}$	0.03	0.06
6. Thickness of the sensing element—$u_{\mathrm{nl,thick}}$	0.002	0.007
7. Measurement instrument—$u_{\mathrm{nl,mi}}$	0.002	0.001
Combined standard uncertainty ($k = 1$)—u_{nl}	0.04	0.08
Expanded uncertainty ($k = 2$)—U_{nl}	0.08	0.16

Assuming that the deviation was a rectangular distribution, the uncertainties for SSPRTs and IPRTs were estimated to be 0.01 °C.

4. Self-heating effect—$u_{\mathrm{nl,self}}$: The fourth component was an uncertainty due to the self-heating for each thermometer. This uncertainty was evaluated by the same method for calibration of the SSPRTs and IPRTs as described in Sect. 2.2. Since the temperature fluctuation of the calibration apparatus was larger than that of the pressure control heat pipe, the component for SSPRTs also became large.
5. Position of the sensing element and Heat flux—$u_{\mathrm{nl,position}}$: The fifth component was evaluated from a temperature profile of the copper cube along a sensing element of the thermometers and effect of a heat flux through a thermometer. They were observed by extracting each thermometer from the center of the copper cube to the position at 30 mm. And then, we calculated same difference of temperature between the center of cube and the position at 15 mm, which was the length of sensing element for each thermometer. The temperature differences for SSPRT and IPRT were within 0.05 °C and 0.1 °C, respectively. Assuming the width of the temperature profile within the sensing elements was a rectangular distribution, the components for the SSPRTs and IPRTs were estimated to be 0.03 °C and 0.06 °C, respectively.
6. Thickness of the sensing element—$u_{\mathrm{nl,thick}}$: The sixth component was caused by a temperature gradient inside each thermometer due to the vertical temperature profile of the copper cube. The temperature gradients inside the SSPRTs and IPRTs were estimated by multiplying the diameter of the thermometers and the temperature gradient of the copper cube. Assuming the temperature gradient was a rectangular distribution, the uncertainties for the SSPRTs and IPRTs were 0.002 °C and 0.007 °C, respectively.
7. Measurement instrument—$u_{\mathrm{nl,mi}}$: The last component was the uncertainty due to measurement instrument as described in Sect. 2.2.

The uncertainties at around 50 °C and 100 °C were obtained in the same manner and were almost the same as those at around 150 °C.

Table 3 Uncertainty of the reference surface temperatures estimated by using five SSPRTs (ID 1–ID 5) and one IPRT (ID B), $t_{1-5+B,}$ and by using two IPRTs (ID A and ID B), $t_{A,B}$, at around 150 °C

Uncertainty component (°C)	t_{1-5+B}	$t_{A,B}$
Propagation of uncertainty due to extrapolation—$u_{enl,prop}$	0.03	0.12
Temperature profile of the surface—$u_{enl,profile}$	0.006	0.006
Combined standard uncertainty ($k = 1$)—u_{enl}	0.04	0.13
Expanded uncertainty ($k = 2$)—U_{enl}	0.08	0.26

As shown in Fig. 4, the temperature profiles inside the copper cube decreased linearly from the lower part to the upper surface. The linear temperature profiles suggest that the heat conduction inside the copper cube can be regarded as a one-dimensional steady state. Based on the one-dimensional steady-state heat conduction, the upper surface temperature (i.e., depth = 0 mm) of the calibration apparatus was estimated by linear extrapolation of the temperature profile of the copper cube. To estimate the upper surface temperature, the linear extrapolation was first performed at the two measurement points of the IPRTs ID A and ID B. This estimation is referred to as $t_{A,B}$ in this study. We also estimated the upper surface temperature by linear extrapolation using the six measurement points of five SSPRTs (ID 1–ID 5) and one IPRT (ID B). This estimation is referred to as t_{1-5+B}. Figure 4 also shows the estimated surface temperatures $t_{A,B}$ and t_{1-5+B} at 0 mm. The error bar is the expanded uncertainty ($k = 2$) for the estimation of the reference surface temperature, the budget of which was presented in Table 3. The estimated temperatures $t_{A,B}$ and t_{1-5+B} agree well within the expanded uncertainty.

The uncertainty components of Table 3 for the estimation of $t_{A,B}$ and t_{1-5+B} are as follows:

1. Propagation of uncertainty due to extrapolation – $u_{enl,prop}$: The first component was estimated by propagation of the measurement uncertainties for SSPRTs and IPRTs described in Table 2.
2. Temperature profile of the surface—$u_{enl,profile}$: The second component was estimated from the temperature profile of the upper surface, which was evaluated from the measured values of three SSPRTs (ID 1, ID 6, and ID 7) inserted in parallel just below the upper surface. Since the difference within ±40 mm on the surface was 0.04 °C, the temperature distribution within ±6 mm (i.e., radius of the surface thermometer) was estimated to be within 0.01 °C. Assuming the difference is a rectangular distribution, the uncertainty was estimated to be 0.006 °C.

The uncertainties of the estimated $t_{A,B}$ and t_{1-5+B} at around 50 °C and 100 °C were obtained in the same way and were almost the same as that at around 150 °C.

3.2 Transient Response of the Temperature Profile of the Copper Cube Through the Surface Thermometer Touching on the Calibration Apparatus

Figure 5 shows the transient response of the temperature profile of the copper cube through the surface thermometer touching on the calibration apparatus at around

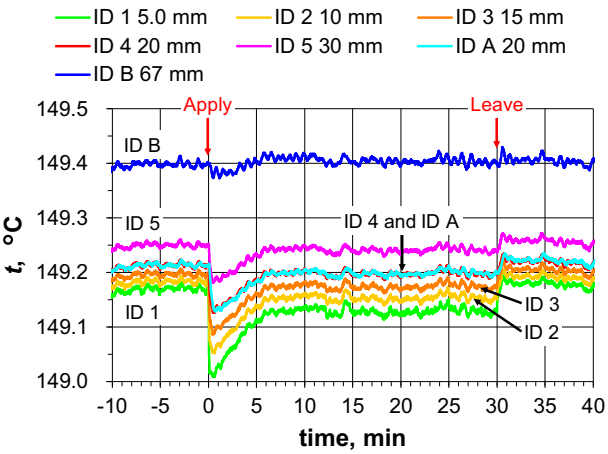

Fig. 5 Transient response observed by IPRT ID A and five SSPRTs (ID 1–ID 5) embedded within the copper cube after the surface thermometer was applied on the upper surface of the copper cube. The surface thermometer was touched at 0 min and leaved at 30 min

150 °C. The surface thermometer was applied to the upper surface from 0 to 30 min. The surface thermometer had been kept at the ambient temperature before being applied to the calibration apparatus.

Temperatures observed by the IPRT ID A and the five SSPRTs (ID 1–ID 5) dropped just after the contact surface thermometer touched on the upper surface. Then, temperature observed by each thermometer started to increase with passing time and finally reached a stable state after about 10 min. On the other hand, variation of temperature observed by the IPRT ID B, which was at the deepest position from the upper surface and at the same position of the temperature control thermometer, was obscure just after the contact surface thermometer touched on the upper surface. Temperature of the IPRT ID B slightly decreased around 2 min. This was probably due to compensation for the temperature drop by a large heat capacity of the copper cube and by controlling temperature at the same position of the IPRT ID B.

Figure 6a, b shows the temperature profile inside the copper cube at 0 s, 3 s, 6 s, 1 min, 3 min and 10 min after the surface thermometer was applied to the upper surface. The temperature profile in Fig. 6a was observed by the five SSPRTs (ID 1–ID 5) and IPRT ID B. The temperature profile in Fig. 6b was observed by the two IPRTs (ID A and B). The data at 0 s were in the no-load state without anything on the reference surface. The temperature observed at 5 mm from the upper surface dropped immediately after the surface thermometer touched on the upper surface. The temperature drop decreased with increasing distance from the upper surface, and thus, the features of the temperature profile became a round shape. Then, the curvature of the round shape became smaller with passing time, and the temperature profile finally showed linear dependence after around 10 min.

This suggests that the heat conduction inside the copper cube reached a one-dimensional steady state again after around 10 min. Therefore, the upper surface temperature of the calibration apparatus after around 10 min was estimated well by

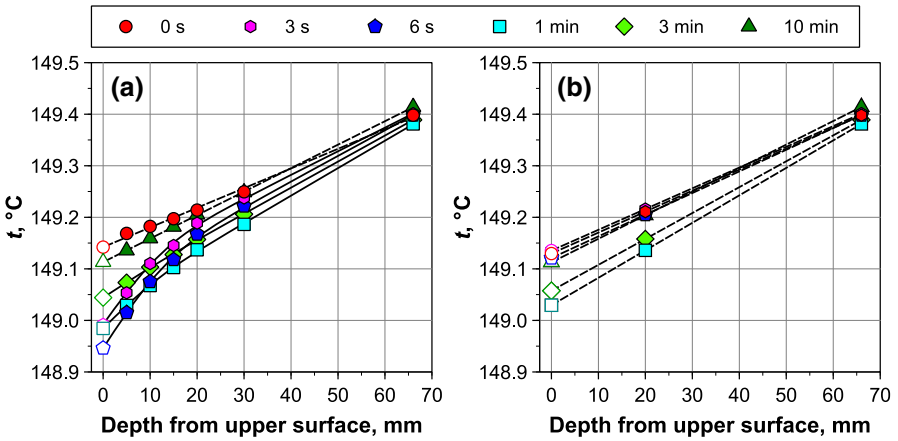

Fig. 6 Temperature profile within the copper cube obtained by using (a) five SSPRTs (ID 1–ID 5) and IPRT ID B and (b) two IPRTs (ID A, B) before and after the contact surface thermometer was applied. The solid lines are fitting curves obtained by using the error function in the same way as one-dimensional transient heat conduction problems. The *dashed lines* are the *linear lines* obtained by the linear regression of the data. The surface temperatures estimated by using five SSPRTs (ID 1–ID 5) one IPRT (ID B), t_{1-5+B}, and by using two IPRTs (ID A and ID B), $t_{A,B}$, are also shown at 0 mm and by *outlined symbols*.

a linear extrapolation in the same manner as that described for the no-load state in Sect. 3.1. The temperature difference between the surface temperatures estimated for the non-load state and the steady state after around 10 min was less than 0.05 °C.

On the other hand, the curvature of the temperature profile was a similar temperature profile inside a material, which is put between two objects with different temperatures, in a one-dimensional transient heat conduction problem. To estimate the upper surface temperature from the curvature of the temperature profiles, we used the error function erfc (x) in the same way as one-dimensional transient heat conduction problems [15] up to 10 min. The upper surface temperature t_{1-5+B} was estimated by extrapolation using the following equation:

$$t_{1-5+B} = a_1 d + a_2 - a_3 \mathrm{erfc}\,(a_4 d)\,, \tag{2}$$

where a_1, a_2, a_3, a_4 are constant terms and d is the distance from the upper surface. The constant terms were estimated by least-squares fitting using the data of the five SSPRTs (ID 1–ID 5) and the IPRT ID B. The solid line in Fig. 6a indicates the fitting curve obtained by using Eq. 2 at 3 s, 6 s, 1 min and 3 min. We obtained good agreement between the curvature of the temperature profiles and the results estimated from Eq. 2. The estimated surface temperature t_{1-5+B} by using Eq. 2 is also shown in Fig. 6a at 0 mm.

We also estimated the upper surface temperature by linear extrapolation using the data of the two IPRTs ID A and ID B in the same manner as described for the non-load state. The dashed lines in Fig. 6b are the linear lines obtained by the linear regression of the data. The estimated surface temperature, $t_{A,B}$, is also shown in Fig. 6b at 0 mm.

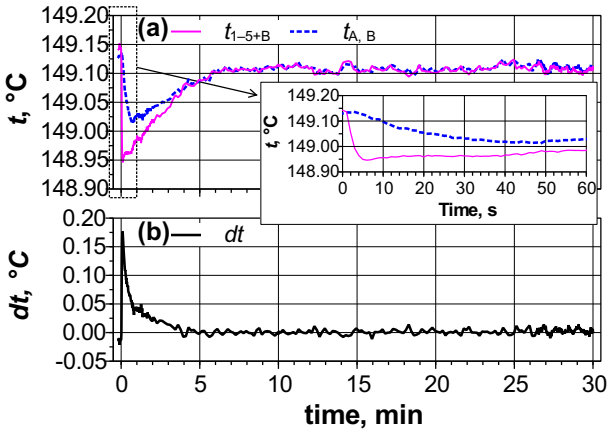

Fig. 7 (a) Changes in the estimated surface temperatures $t_{A,B}$ and t_{1-5+B}. (b) Difference of temperature $dt = t_{A,B} - t_{1-5+B}$. Inset of Fig. 7a is enlarged from 0 s to 60 s

Figure 7a shows a change in the estimated surface temperatures $t_{A,B}$ and t_{1-5+B} with passing time. Figure 7b shows the difference between $t_{A,B}$ and t_{1-5+B}, which is designated as $dt(= t_{A,B} - t_{1-5+B})$. The temperature t_{1-5+B} markedly dropped just after the surface thermometer touched on the reference surface and showed a minimum value at around 5 s, which was 0.2 °C lower than that estimated just before the surface thermometer was applied. Then, t_{1-5+B} gradually increased and finally reached a stable value after around 10 min. On the other hand, the temperature $t_{A,B}$ also dropped just after the surface thermometer touched on the reference surface, but the temperature drop of $t_{A,B}$ was apparently smaller than that of t_{1-5+B}. The temperature $t_{A,B}$ started to increase after around 1 min and reached a similar value as t_{1-5+B} after around 5 min.

As shown in Fig. 7b, the temperature differencedt between $t_{A,B}$ and t_{1-5+B} shows a sharp peak and then decreases with passing time. It finally became negligible at around 5 min. These results imply that the estimation of the surface temperature by linear fitting will show some discrepancy from the surface temperature estimated by much more detailed temperature profile of the copper cube in the transient state. Thus, our results suggest that an uncertainty component due to the temperature differencedt is required for estimation of uncertainty of the reference temperature obtained by the linear extrapolation using two IPRTs in the transient state.

Table 4 presents the uncertainty budget for estimating the surface temperature by using $t_{A,B}$ in both the transient and the steady states. The uncertainty budget for the steady state was the same as that given in Table 3 for the non-load state. On the other hand, the uncertainty components for the transient state were estimated in the same way as those for the non-load state except for the uncertainty component due to the difference dt between $t_{A,B}$ and t_{1-5+B} ($u_{ets,diff}$). As shown in Fig. 7b, the temperature difference dt, was within 0.2 °C, even at several seconds after the contact surface thermometer touching on the reference surface. Assuming a rectangular distribution, the uncertainty component $u_{ets,diff}$ was estimated to be 0.12 °C. Thus, the expanded

Table 4 Uncertainty of the reference surface temperatures estimated by using two IPRTs (ID A and ID B), $t_{A,B,}$ for the transient and steady state after the surface thermometer was applied to the upper surface at around 150 °C

Uncertainty of component (°C)	$t_{A,B}$	
	Transient state	Steady state
Propagation of uncertainty due to extrapolation—$u_{ets,prop}$	0.12	0.12
Difference between t_{1-5+B} and $t_{A,B}$—$u_{ets,diff}$	0.12	–
Temperature profile on the surface—$u_{ets,profile}$	0.02	0.006
Combined standard uncertainty ($k = 1$)—u_{ets}	0.18	0.13
Expanded uncertainty ($k = 2$)—U_{ets}	0.36	0.26

uncertainty for estimation of the surface temperature was 0.36 mK in the transient state.

Industries prefer to use a simple way for estimation of the reference temperature for calibration or check of contact surface thermometers. They also mostly prefer to calibrate or check the contact surface thermometers within ±1 °C of accuracy at around 150 °C. Therefore, our results indicates that the calibration apparatus developed in this study provides enough capability for calibration or check of contact surface thermometers in industrial fields even when the reference temperature estimated by linear extrapolation using two IPRTs.

3.3 Comparison Between the Upper Surface Temperature and Output Value of the Surface Thermometer

In this study, our main scope was estimating the surface temperature of our calibration apparatus, but we also tried to check the relationship between the upper surface temperature of our calibration apparatus and the output value of the contact surface thermometer during measurement.

Figure 8 shows the relative differences in temperature from a stable state (over 10 min) for t_{1-5+B} and $t_{A,B}$ and the output value of the surface thermometer, which was converted to the temperature from the voltage. These are referred to as dt_{1-5+B}, $dt_{A,B}$, and dt_{TC}, respectively.

As shown in Fig. 8, dt_{TC} was over −0.5 °C at first. Then, the difference was suppressed with passing time. Finally, dt_{TC} showed the same trend as dt_{1-5+B} and $dt_{A,B}$ over 10 min.

Assuming that the contact surface thermometer shows the same temperature of the reference surface in the steady state over 10 min, we tried to estimate the difference in temperature between the surface thermometer and the reference surface by $dt_{TC} - dt_{1-5+B}$. Figure 9 shows the $dt_{TC} - dt_{1-5+B}$ obtained by different six runs. Tests $1 - i (i = 1$ to 4) and $2 - j (j = 1, 2)$ were performed on different days. All of the data agreed within ±0.05 °C in the steady state, indicating good repeatability of the measurements. The temperature difference $dt_{TC} - dt_{1-5+B}$ reached −0.4 °C at 5 s and then increased with passing time. It was within −0.1 °C after 3 min. Finally,

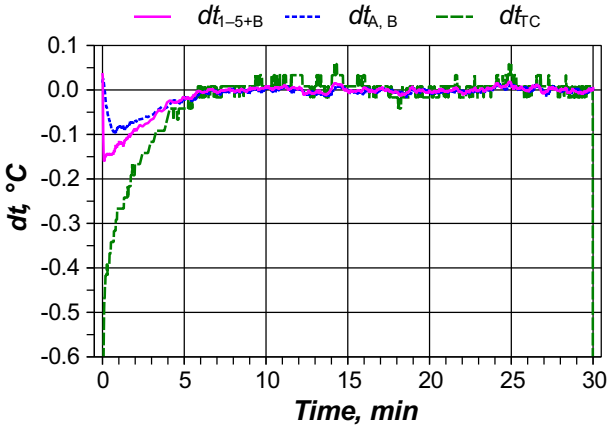

Fig. 8 Relative differences in temperature from a stable state for t_{1-5+B} and $t_{A,B}$ and the output voltage of the surface thermometer, which is converted to the temperature. These are referred to as dt_{1-5+B}, $dt_{A,B}$, and dt_{TC}, respectively

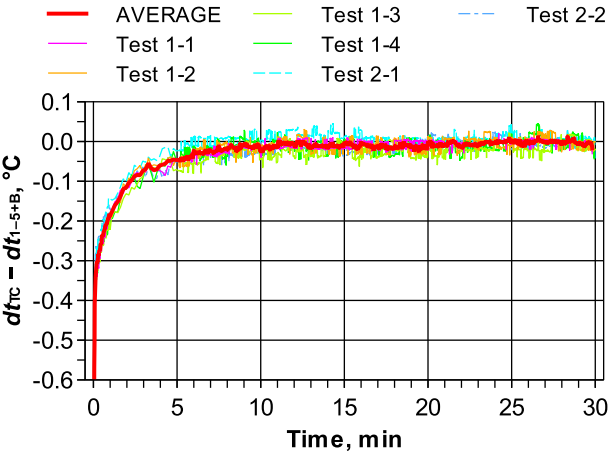

Fig. 9 Temperature difference between dt_{TC} and dt_{1-5+B} observed by six different runs: tests $1-i\,(i = 1to4)$ and $2-j\,(j = 1, 2)$ were measured on different days.

the difference $dt_{TC} - dt_{1-5+B}$ became negligible after 10 min. This indicates that the temperature difference between the surface thermometer and upper surface existed at a time of less than 10 min. This suggests that the uncertainty component due to the temperature difference between the surface thermometer and upper surface is required for the estimation of uncertainty for calibration of surface thermometers, especially in the transient state.

4 Conclusion

In this study, the upper surface temperature of the copper cube in the calibration apparatus was estimated by using SSPRTs with a diameter of 1 mm and conventional

IPRTs with a diameter of 3.2 mm at around 50 °C, 100 °C, and 150 °C for a no-load state without anything on the upper surface. We also estimated the upper surface temperature through the surface thermometer was applied to the upper surface at around 150°C.

In the no-load state, the temperature profiles inside the copper cube decreased linearly from the inside to the surface. This suggests that the heat conduction inside the copper cube can be regarded as a one-dimensional steady state and the surface temperature can be estimated by linear extrapolation.

In the transient state after the surface thermometer touched on the upper surface, the temperature profile became a round shape. The curvature of the round shape became smaller with passing time, and the temperature profile finally showed linear dependence after around 10 min, indicating the upper surface temperature of the calibration apparatus after around 10 min was estimated well by a linear extrapolation in the same reason for the no-load state. In the transient state just after the surface thermometer touched on the upper surface, we also obtained good agreement between the curvature of the temperature profiles and the results estimated by using an error function in the similar manner as that used for a one-dimensional transient heat conduction problem. Although the temperature profile is a curvature in the transient state, estimation of the reference surface temperature using a linear extrapolation is preferable for most of industrial fields because of its simple way. In this study, the temperature difference between the estimated temperature by linear extrapolation and that by the method of using the error function was within 0.2 °C in the transient state. Taking into account of the temperature difference, the expanded uncertainty of the reference surface temperature estimated using two IPRTs was0.4 °C in the transient state. Since most of the industries prefer to calibrate or check the contact surface thermometers within ±1 °C of accuracy, this indicates that estimation of the reference temperature using two IPRTs of our calibration apparatus has enough capability for industrial usage not only in the steady state but also in the transient state.

In this study, we also checked the relationship between the estimated surface temperature and the output of the surface thermometer. A temperature difference between the surface thermometer and upper surface was estimated to be over 0.1 °C at several minutes after the surface thermometer touching on the reference surface. This suggests that the uncertainty component due to the temperature difference between the surface thermometer and the upper surface is required for estimation of an uncertainty in the transient state.

In this study, the temperature range was limited up to 150 °C and the estimation of the reference surface temperature of the calibration apparatus was evaluated by using only one type of contact surface thermometers. Our future plan is to apply the technique for the estimation of the reference surface temperature at other temperatures, especially over 150 °C, and also for calibration of other types of contact surface thermometers.

Acknowledgements We thank Anritsu Meter Co., Ltd. for their cooperation in developing and providing the surface thermometer and dedicated device for this study. We also thank members of the thermometry and frontier thermometry sections in NMIJ/AIST for the valuable discussions.

References

1. H. Preston-Thomas, Metrologia **27**, 3 (1990). doi:10.1088/0026-1394/27/1/002
2. M. de Groot, High Temp. Press. **29**, 591 (1997). doi:10.1068/htps3
3. F. Bernhard, S. Augustin, H. Mammen, K.D. Sommer, E. Tegeler, M. Wagner, U. Demisch, in *Proceedings of TEMPMEKO '99, 7th International Symposium on Temperature and Thermal Measurements in Industry and Science,* ed. by J.F. Dubbeldam (NMi Van Swinden Laboratorium, Delft, 1999), pp. 257–262
4. R. Morice, E. András, E. Devin, T. Kovács, in *Proceedings of TEMPMEKO 2001, 8th International Symposium on Temperature and Thermal Measurements in Industry and Science,* ed. by B. Fellmuth, J. Seidel, G. Scholz (VDE-Verlag, Berlin, 2001), pp. 1111–1116
5. E. András, in *Proceedings of XVII IMEKO World Congress, Metrology in the 3rd Millennium,* ed. by D. Ilic, M. Borsic, J. Butorac (HMD - Croatian Metrology Society, Dubrovnik, 2003), pp. 1598–1603
6. E. András, Report of EUROMET Project No. 635 (2003)
7. M. Lidbeck, J. Ivarsson, E. András, J.E. Holmen, T. Weckström, F. Andersen, Int. J. Thermophys. **29**, 414 (2007). doi:10.1007/s10765-007-0303-y
8. F. Yebra, H. González-Jorge, L. Lorenzo, M. Campos, J. Silva, F. Troncoso, J. Rodríguez, Metrologia **44**, 217 (2007). doi:10.1088/0026-1394/44/3/008
9. L. Rosso, N. Koneva, V. Fernicola, Int. J. Thermophys. **30**, 257 (2008). doi:10.1007/s10765-008-0495-9
10. F. Arpino, V. Fernicola, A. Frattolillo, L. Rosso, Int. J. Thermophys. **30**, 306 (2009). doi:10.1007/s10765-008-0451-8
11. G. Beges, M. Rudman, J. Drnovsek, Int. J. Thermophys. **32**, 396 (2010). doi:10.1007/s10765-010-0903-9
12. B.E. Adams, A.M. Hunter, in *Temperature: Its Measurement and Control in Science and Industry*, vol. 8, ed. by C.W. Meyer (AIP Publishing LLC, New York, 2013), pp. 909–914. doi:10.1063/1.4819665
13. K. Yamazawa, K. Anso, J.V. Widiatmo, J. Tamba, M. Arai, Int. J. Thermophys. **32**, 2397 (2011). doi:10.1007/s10765-011-1040-9
14. J. Tamba, I. Kishimoto, M. Arai, in *Temperature: Its Measurement and Control in Science and Industry*, vol. 7, ed. by D.C. Ripple (AIP PRESS, New York, 2003), pp. 963–968. doi:10.1063/1.1627253
15. Japan Society of Mechanical Engineers, in *JSME Data Book: Heat Transfer*, 5th edn., ed. by Shigefumi NISHIO (Japan Society of Mechanical Engineers, Japan, 2009)